An edge detection algorithm matching visual contour perception

A. T. Mohammed
Astronomy Department, College of science, University of Baghdad
Al-Jadiryia, Baghdad, Iraq.

Abstract

For several applications, it is very important to have an edge detection technique matching human visual contour perception and less sensitive to noise. The edge detection algorithm describes in this paper based on the results obtained by Maximum a posteriori (MAP) and Maximum Entropy (ME) deblurring algorithms. The technique makes a trade-off between sharpening and smoothing the noisy image. One of the advantages of the described algorithm is less sensitive to noise than that given by Marr and Geuen techniques that considered to be the best edge detection algorithms in terms of matching human visual contour perception.

1. Introduction:

In all applications where images are processed for ultimate evaluation by a human observer, it is important to have an edge detection technique which matched visual contour perception and created as small false edges as possible. Two techniques which proved to be the best edge detectors in the sense that they are matched human visual contour perception. The first is Marr et. al [1] and the second is given by Geuen [2]. These techniques are very sensitive to noise. The algorithm which developed in this paper is applied for a variety of images and the results are compared with that using [1] and [2].

2. Filter design:

Most of the image degradations do involve blurring and introduction of the noise. Blurring weakens high spatial frequencies more than lower ones; this suggests that images can be sharpening by emphasizing their high spatial frequencies. This type of sharpening are used when the signal-to-noise ratio is very high. Otherwise, the noise become the dominant features in the restored image [3,4].

It has been shown from the results obtained via MAP and ME [5] deblurring algorithms for images corrupted by noise, the intermediate frequency components were enhanced and a certain level of high frequency components were suppressed because at this level, noise is dominant and contain very small information of the object of interest as shown in Fig.(1). This figure demonstrate the row summed power spectra of the restored real image of a radio Galaxy NGC 6240 by MAP and ME algorithms (for more details, see [5]). Therefore, the objective of this section is to find a filter which sharpen the features and suppress the noise. In the presence of noise, MAP and ME enhance the intermediate frequency components and attenuate a certain level of high frequency components. The filter design which based on its assumption is taken to be the (Fourier modulus) of the second derivative of the Gaussian function.

$$G(r) = \frac{-1}{\pi\sigma^4}\left[1 - \frac{r^2}{2\sigma^2}\right] \cdot e^{\frac{-r^2}{2\sigma^2}} \quad ...(1)$$

Where **r** is the distance from the origin (x_o,y_o) to the point (x,y) of the two dimensional array.

The Gaussian function has been chosen because it is rotationally symmetric, and is suitable for localizing frequencies at the lower and intermediate end of the spectrum. Fig.(2) shows the two-dimensional plot of the (Fourier modulus) of equation (1) at $\sigma = 2$. It should be pointed out here that this filter is a standard deviation dependent filter. Changing a of this filter affects certain level of low, intermediate and high frequency components. This filter was chosen because it is design to sharpen the features by performing inverse filtering and smoothing the noise by attenuating a certain level of high frequency components all depends on the parameter a of equation (1).

3. The edge detector:

Geuen edge detector [2] based on the assumption that the low pass filter are realized by calculating the mean value within rectangular windows of different sizes in the spatial domain. The characteristic of the band pass filter is the result of the structure of low pass filter, each having a different window size. The new edge detector can be performed as before but multiplying the filter shown in Fig.(2) of a certain value of a with the Fourier transform of the image of interest. The filter shown in Fig.(2) is a Fourier domain filter. Each filter can be realized by defining a of the second derivative of the Gaussian function as given by equation (1). The two images obtained from these two filters (i.e. multiplying each filter with the Fourier transform of the image to be detected) are subtracted from each other to obtain the band-pass filtered image of interest or the two filters output obtained using two values of a can be subtracted to get the new filter output (examples of subtracted two filters output is shown in Fig.(3) which can be multiplied with the
Fourier transform of the image to be detected. The zero-crossing technique should then be performed to detect the possible contour points. The block diagram of the new edge detection technique is illustrated in Fig.(4).

The zero crossing is defined as possible contour points. For the detection of zero-crossing only a change in filter output sign, regarding the four connected neighborhood, has to be recognized. In the case of the Marr et. al. and Geuen techniques, performing zero crossing on low constraints noisy area will always generate false contour points while with the new technique the false points are reduced greatly. Fig.(5) show central lines through the filter output of the real image of Saturn using the three techniques. The low contrast area is presented a pure background noise. The Marr and Geuen techniques produced zero-crossing points at this area while the new technique produce no zero-crossing points because there is no change in sign at this background noisy area.
In order to make Marr and Geuen techniques, more efficient by detection as small false edge points as possible, we suggest performing a threshold value. Looking back to Fig.(5), the change in the values of the background noise is very small, so that a threshold value should set up to reject these false edge points.

4. Comparison results:

In this section, the applications of the two edge detection techniques [1,2] and the new one for variety of images are presented. Fig.(6a) demonstrates the real image of Saturn. Fig.(6b) show the edge detected images via the new technique. Fig.(6c) show the results obtained via the Marr technique using different values of σ . Fig.(6d) show the results obtained via the Geuen technique using different window sizes. Comparing those results, it is clearly seen that the Marr and Geuen techniques are very sensitive to noise. Increasing σ with the Marr technique and window size with the Geuen technique, noise points (false edges) are smoothed out but on the expense of suppressing essential edge points. However, the results obtained from the new technique show great noise suppression and not on the expenses of suppressing fundamental edge points. Fig.(7) demonstrate the results of using another image. Fig.(7a) shows a test image., The detected image by the new technique is shown in Fig.(7b). The edge detected images via both the Marr and Geuen techniques are shown in Fig(7c & d) respectively. Note that all the fundamental edge points are detected in all cases but the new technique create as small false edges as possible.

It is important to have quantitative quality measure to judge the performance of a given technique. However, since the three edge detection techniques are matched visual contour perception, then all quantitative measure is a good one for judging the performance.

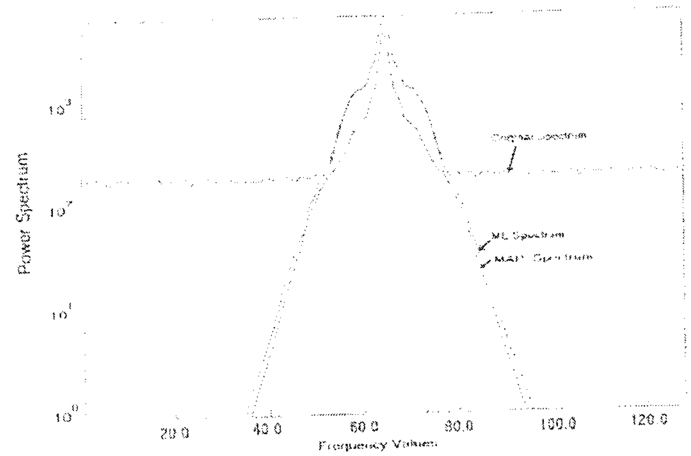

Fig.(1): Row summed power spectra of the restored images of A real radio Galaxy NGC 6240 by MAP and ME deblurring algorithms.

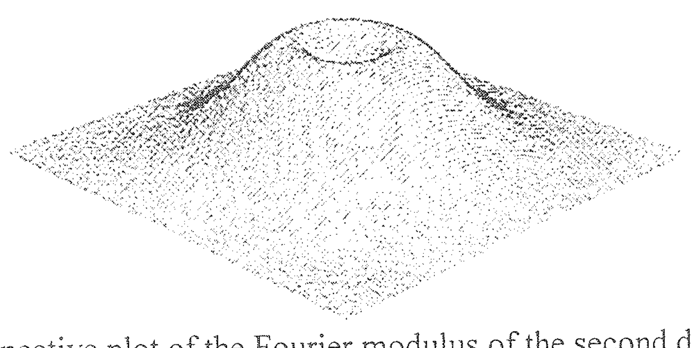

Fig.(2): Perspective plot of the Fourier modulus of the second derivative of a Gaussian function with $\sigma = 2$.

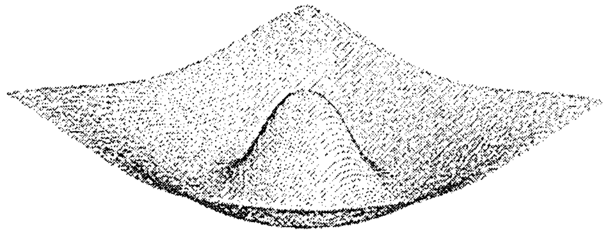

Fig.(3): Subtracted two filters obtained following Fig.2, using $\sigma_1 = 1.3$ and $\sigma_2 = 3.3$

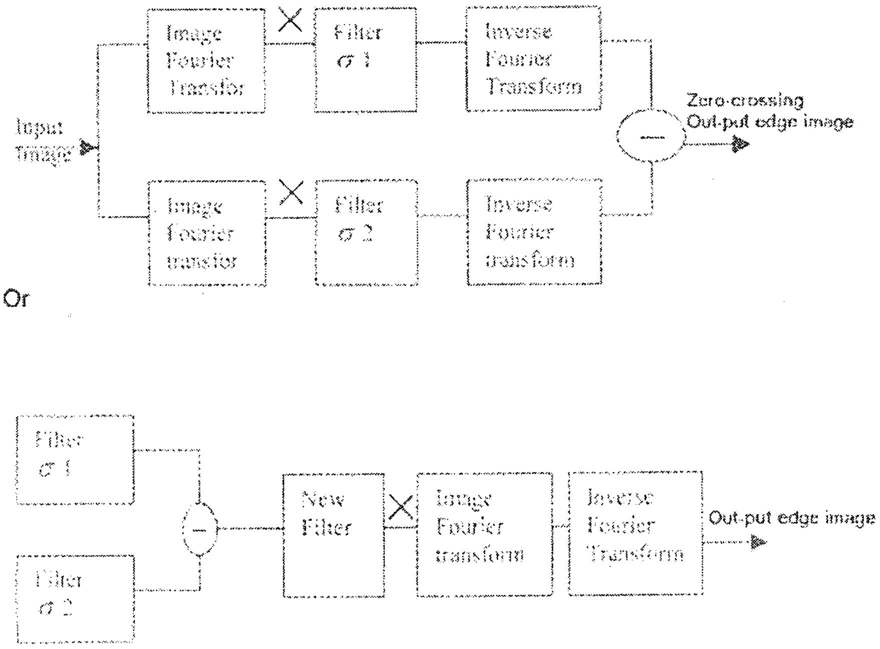

Fig.(4): Block diagram of the new edge detection technique.

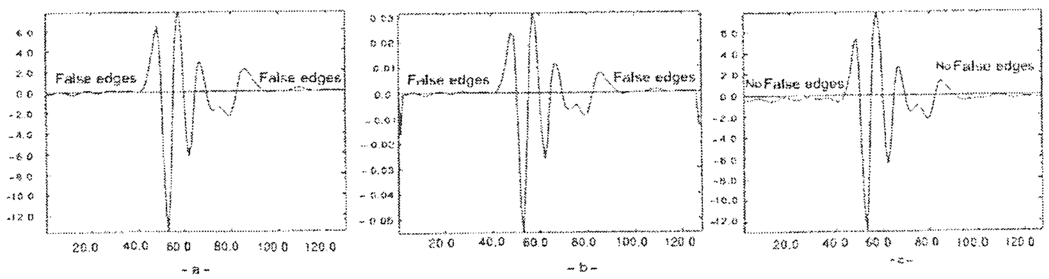

Fig.(5): Central line through the images obtained by the three techniques, before performing zero-crossing: a- Marr-technique with $\sigma = 1$, b-Geuen-technique with window sizes 3×3 and 5×5 pixels, c-New technique with $\sigma_1 = 1.3$ and $\sigma_2 = 3.3$

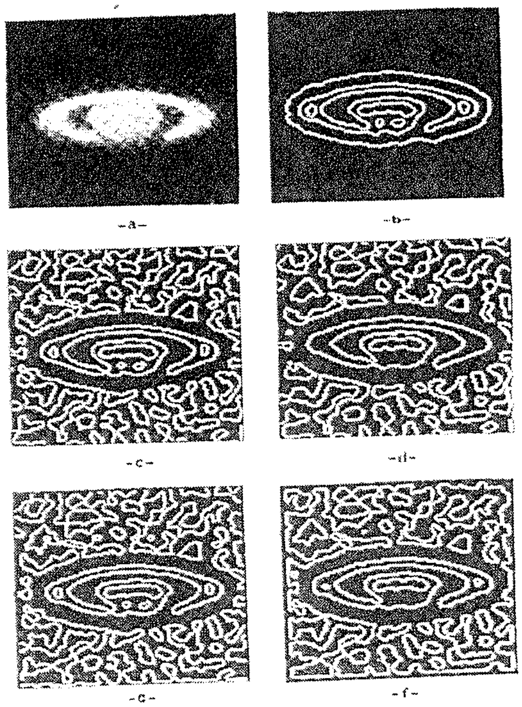

Fig.(6): Edge detected images of Saturn., a- Real image of Saturn, b- Edge image obtained via the new technique with $\sigma_1 = 1.3$ and $\sigma_2 = 3.3$., c&d- Edge images obtained via Marr technique with $\sigma_1 = 1$& 3., e & f- Edge images obtained via Geuen technique with window sizes 3×3 and 5×5 pixels and 3×3 and 9×9 pixels

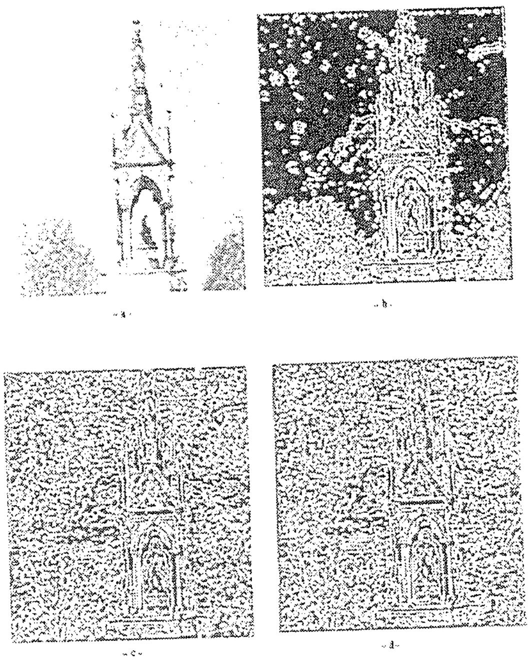

Fig.(7): Edge results performed on sampled of real images, a-Image sample, b- New technique with $\sigma_1 = 1.3$, c- Marr with $\sigma = 1$, and d- Geuen by 3×3 and 5×5 windows

5. Conclusions:

The structure of the described edge detection technique is quit simple, matches human visual contour perception and less sensitive to noise. The results are better than those given by [1 & 2] which are known as the best algorithms so far. The technique can easily be implemented on different computer systems or to be used for hardware applications.

References:

[1] Marr D. and Hildreth E. (1980). Proc. R. Soc. Lond. 207, p.187.

[2] Geuen W. (1 983)."A fast edge detection algorithm matching visual contour perception". In image sequence processing and dynamic scene analysis. NATO AST series. Ed. By Huang T. S., F-2, p.483.

[3] Rosenfeld A. and Kak A. C. (1 982)."Digital picture processing", Vol.2.

[4] S.E.Umbaush,1998 "Computer Vision and Image Processing.", a practical approach using CVIP tools.

[5] Mohammed A. T. (1987)."Reconstruction and enhancement of astronomical objects by image processing", Ph.D. Thesis, University of London , , King's college.